ISSN 0001-4370, Oceanology, 2009, Vol. 49, No. 2, pp. 166–181. © Pleiades Publishing, Inc., 2009.
Original Russian Text © L.I. Lobkovsky, A.B. Rabinovich, E.A. Kulikov, A.I. Ivashchenko, I.V. Fine, R.E. Thomson, T.N. Ivelskaya, G.S. Bogdanov, 2009, published in Okeanologiya, 2009, Vol. 49, No. 2, pp. 181–197.

MARINE PHYSICS

The Kuril Earthquakes and Tsunamis of November 15, 2006, and January 13, 2007: Observations, Analysis, and Numerical Modeling

L. I. Lobkovsky[a], A. B. Rabinovich[a], E. A. Kulikov[a], A. I. Ivashchenko[a], I. V. Fine[b], R. E. Thomson[b], T. N. Ivelskaya[c], and G. S. Bogdanov[d]

[a] *Shirshov Institute of Oceanology, Russian Academy of Sciences, Moscow, Russia*

[b] *Department of Fisheries and Oceans, Institute of Ocean Sciences, Sidney, British Columbia, Canada*

[c] *Tsunami Center, Sakhalin Department of the Federal Service for Hydrometeorology and Environment Monitoring, Yuzhno-Sakhalinsk, 693002 Russia*

[d] *Institute of Marine Geology and Geophysics, Far Eastern Division of the Russian Academy of Sciences, Yuzhno-Sakhalinsk, Russia*

e-mail: abr@iki.rssi.ru; KulikovE@cnt.ru

Received January 28, 2008; in final form, March 27, 2008

Abstract—Major earthquakes occurred in the region of the Central Kuril Islands on November 15, 2006 (M_w = 8.3) and January 13, 2007 (M_w = 8.1). These earthquakes generated strong tsunamis recorded throughout the entire Pacific Ocean. The first was the strongest trans-Pacific tsunami of the past 42 years (since the Alaska tsunami in 1964). The high probability of a strong earthquake ($M_w \geq 8.5$) and associated destructive tsunami occurring in this region was predicted earlier. The most probable earthquake source region was investigated and possible scenarios for the tsunami generation were modeled. Investigations of the events that occurred on November 15, 2006, and January 13, 2007, enabled us to estimate the validity of the forecast and compare the parameters of the forecasted and observed earthquakes and tsunamis. In this paper, we discuss the concept of "seismic gaps," which formed the basis for the forecast of these events, and put forward further assumptions about the expected seismic activity in the region. We investigate the efficiency of the tsunami warning services and estimate the statistical parameters for the observed tsunami waves that struck the Far Eastern coast of Russia and Northern Japan. The propagation and transformation of the 2006 and 2007 tsunamis are studied using numerical hydrodynamic modeling. The spatial characteristics of the two events are compared.

DOI: 10.1134/S0001437009020027

1. INTRODUCTION

On November 15, 2006, at 11:14 UTC, a strong (magnitude M_w = 8.3) tsunamigenic earthquake occurred in the vicinity of the Central Kuril Islands. The epicenter of the earthquake was located at the continental slope of the deep Kuril-Kamchatka Trench, approximately 90 km southeast of Simushir Island (Fig. 1). The earthquake generated a trans-Pacific tsunami that was recorded throughout the entire Pacific Ocean, including the coasts of Japan, the Hawaiian Islands, Alaska, Canada, Peru, Chile, New Zealand, and the west coast of the USA [28, 34, 44, 48]. Fortunately, this tsunami (as well as the earthquake) did not cause any casualties. However, based on the fact that the tsunami spanned the entire Pacific Ocean and impacted regions highly remote from the source (in particular, Crescent City, California, located 6600 km from the epicenter of the earthquake [34, 50]), this tsunami is considered the strongest event of its type to be observed in the Pacific Ocean within the past 42 years since the catastrophic Alaska tsunami of March 28, 1964.

It is worth noting that the tsunami of November 15, 2006 (the First Simushir tsunami) was one of the first major tsunamis in the Pacific Ocean to have occurred in the "instrumental era." It was recorded with high accuracy by numerous digital coastal tide gauges and by deep-water DART[1] stations located in the open Pacific Ocean. The tsunami occurred fewer than two years after the catastrophic earthquake and tsunami of December 26, 2004 in the Indian Ocean, which caused unprecedented destruction and casualties. A consequence of the 2004 event was a marked increase in tsunami research [1, 13, 40, 47, 49]. What makes the earthquake and tsunami of 2006 unique is that the high probability of an imminent event in the region of the Central Kuril Islands was predicted in advance [9, 10, 14], and the likely earthquake source region pre-investigated. Different scenarios for the formation and propagation

[1] DART is an acronym for Deep-Ocean Assessment and Reporting of Tsunamis, a deep-water system of stations deployed by the United States along seismic active regions of the Pacific Ocean to monitor tsunami waves.

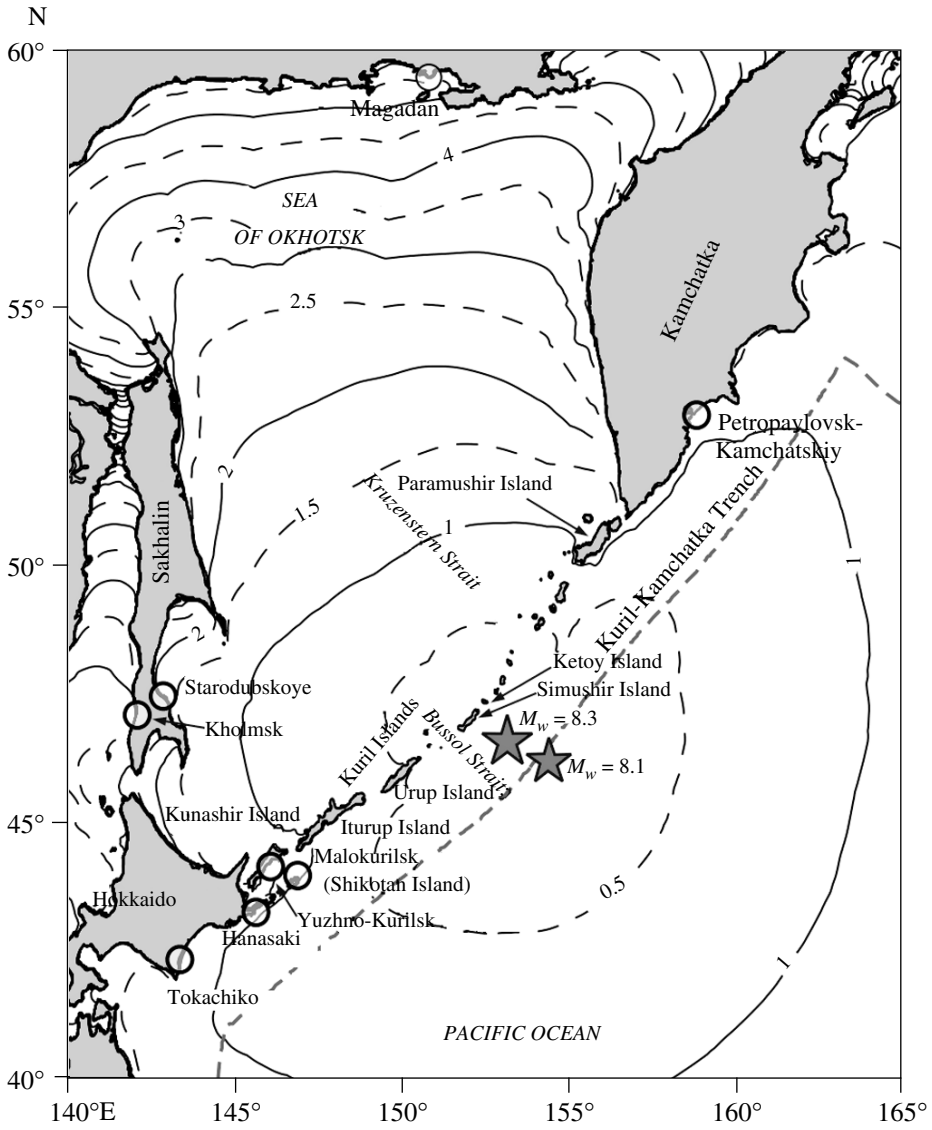

Fig. 1. Map of the deep Kuril-Kamchatka Trench and adjacent regions. Asterisks denote the location of earthquake epicenters for the November 15, 2006 and January 13, 2007 earthquakes; circles denote the location of tide gauge stations; the thick dashed line shows the axis of the trench. Thin solid and dashed lines show calculated isochrones (hours) of the earthquake generated tsunami wave travel time for November 15, 2006.

of tsunami waves were modeled in advance [9, 15, 36]. Thus, for the first time in the field of tsunami research an event began to be investigated before it actually happened.

On January 13, 2007, two months after the November 15, 2006 earthquake, another earthquake of similar magnitude ($M_w = 8.1$) occurred in the region of the Central Kuril Islands (the Second Simushir earthquake). The epicenter of the main shock was located on the oceanic side of the Kuril-Kamchatka Trench approximately 100 km to the east of the epicenter of the earthquake of November 15, 2006 within the limits of the lithospheric plate (Fig. 1). Despite the close proximity of the source zones and doubtless correlation between the two events, the seismic parameters of the second earthquake differed significantly from those of the earlier earthquake. The earthquake of January 13, 2007 also generated a trans-Pacific tsunami, which was reliably recorded in the Kuril Islands, Japan, Hawaii and the Aleutian Islands, as well as at the coasts of Alaska, British Columbia, Oregon, California, Peru, and Chile [28, 44, 48]. However, differences in the seismic source generation mechanisms resulted in marked differences in the tsunami wave parameters, in particular, in the sign of the first wave propagating into the open ocean. This wave was positive for the tsunami of 2006 and negative for the tsunami of 2007.

The earthquake on January 13, 2007 was not predicted, although it might have been possible to foresee this event based on some general considerations: events of this type, consisting of strong repeated shocks following a major earthquake, frequently occur within oceanic plates in subduction zones characterized by strong cohesion between the interacting plates [24]. In general, strong double seismic events are frequent occurrences: for example, the catastrophic earthquake of December 26, 2004 (M_w = 9.3) in the vicinity of North Sumatra (Indian Ocean) was followed by the earthquake of March 28, 2005 (M_w = 8.7) in the same region [1, 40]; and the Urup earthquake of October 13, 1963 (M_w = 8.3) was followed by the earthquake of October 20, 1963 (M_w = 7.9) [18, 26].

The primary objective of the present study is to provide comparative analyses between the earthquakes and tsunamis of November 15, 2006 and January 13, 2007. Attention is mainly focused on the near zone, including regions of the Kuril Islands and Japan. Some results from this analysis are reported in [16].

2. THE CONCEPT OF SEISMIC GAPS AND EARTHQUAKE FORECAST

The catastrophic tsunami of December 26, 2004 in the Indian Ocean was generated by an exceptionally intense earthquake (M_w = 9.3) which, in the history of instrumental observations (from the beginning of the 20th century), was second in magnitude only to the Chilean earthquake of May 22, 1960 (M_w = 9.5) [47]. The earthquake and tsunami of 2004 led to many questions, among which the most frequent ones are probably the following: Why was this earthquake and associated tsunami so strong? Why did the earthquake occur precisely in this particular region near the northwestern coast of Sumatra Island? Where will the next catastrophic earthquake and tsunami occur?

Analysis carried out in 2005 at the Institute of Oceanology, Russian Academy of Sciences (IO RAN) demonstrates that the central and eastern parts of the Sunda Islands Arc in the Indian Ocean have been the source of numerous strong earthquakes within the past 150 years. In contrast, no earthquakes of comparable strength have been observed over the same time period in the northern part of the arc or in the zone of the Nicobar and Andaman Islands that continues the arc to the north (the location of the earthquake source on December 26, 2004). As a result, considerable elastic deformational energy had been accumulating in this region prior to the earthquake. This energy was released on December 26, 2004 [10, 13, 14].

Seismically active regions of the world are located mainly near island arcs and ocean margins. Subsets of these regions where strong earthquakes have not occurred for considerable time (the so-called "zones of seismic silence" or "seismic gaps") have a high probability for a catastrophic earthquake [21, 37, 38]. The enormous elastic energy that has accumulated in these zones as a result of long-term interaction between lithospheric plates is ready to release at any moment. An effective method for the long-term forecasting of strong earthquakes and related tsunamis is based on locating of seismic gaps and then estimating their seismic potential [12, 21]. For example, the authors of [43] found a major seismic gap located between 15° and 24°S on the basis seismic data for the coast of South America from 1552 to 1999. Strong earthquakes occurred repeatedly in this region (namely in 1604, 1705, 1868, and 1877) and were accompanied by destructive tsunamis (with wave heights from 8 to 24 m). The authors of [43] suggested that a tsunamigenic event was imminent for this region and wrote that "……This region has high potential for a major earthquake of magnitude greater than 8.0…Tsunamis with wave heights of about 16 m … are likely to occur in the near future". The article was submitted in March 2001; three months later on June 23, 2001, a catastrophic earthquake occurred in this region (M_w= 8.4). The recorded tsunami runup at the coast from this event exceeded 9 m [8, 35].

Investigation of zones of high seismic risk in the Pacific Ocean show that one of the largest and most persistent seismic gaps is located in the central sector of the Kuril-Kamchatka subduction zone. According to the seismic tectonic characteristics of the region, this gap is similar to the one which existed up to December 2004 in the northern part of the Sunda Arc [9, 10, 13, 14]. The existence of three seismic gaps in the Kuril-Kamchatka zone (southwestern, northeastern, and central) was determined by S.A. Fedotov more than 40 years ago [20]. By 2005, the first two gaps had experienced strong earthquakes over the period 1965–2004 (Fig. 2), while the central gap continued to be "silent". This gap, which extended in the northeastern direction more than 300 km beginning from the southern extremity of Simushir Island, was bounded in the southwest by the source region for the intense earthquake of 1918 and in the northeast by the source region for the earthquake of 1915 (Fig. 2). Strong earthquakes within the gap had not occurred for more than 150 years. According to the data in [21], the characteristic duration of seismic cycles in this zone is 140 ± 60 years. As emphasized in [9, 10, 14], the probability of a catastrophic earthquake and related tsunami within the Central Kuril seismic gap is therefore extremely high. This region requires active research and permanent geophysical monitoring.

During August to September 2005 and 2006, the Russian Academy of Sciences organized two geophysical expeditions onboard the R/V *Akademik Lavrentiev* to study the seismic gap. During these expeditions, the structure of the subduction zone in the vicinity of the Central Kuril gap was studied, regions of transversal fractures were distinguished, and seismic, gravimetric, magnetic, and bathymetric profiling of the region were carried out (the main results of the 2005 expedition are presented in [10]). The investigations carried out during these two expeditions confirmed the high seismic

potential of the central part of the Kuril Islands Arc and demonstrated that the zone is divided by transversal fractures into a series of small blocks (like keys on a keyboard). On this basis, the strength of the anticipated earthquake depends on the number of "keys" acting simultaneously. A specified key model for earthquake occurrence in subduction zones was used for prognostic calculations of the resulting tsunami [12]. Different versions of the key motions were considered and different scenarios of the possible source were analyzed [9, 15, 36].

As forecast, the earthquakes of November 15, 2006 and January 13, 2007 occurred exactly within the Central Kuril gap (Fig. 2). Therefore, the situation with respect to the Simushir earthquakes and tsunamis in 2006 and 2007 is quite unique: strong earthquake and tsunami were predicted, two expeditions were carried out in the forecasted source zone during the period preceding these events, and the results of these expeditions were used to construct prognostic models of earthquakes and tsunamis.

3. PROGNOSTIC TSUNAMI MODELING IN THE CENTRAL KURIL ISLANDS REGION

Numerical modeling of possible destructive tsunamis due to a source located in the Central Kuril Islands region was conducted for the northwestern part of the Pacific Ocean including the Sea of Okhotsk [9, 36]. The computational domain was delineated by the rectangle 40.0°–60.0°N, 140.0°–165.0°E (Fig. 1). The ETOPO-6.2 [46] bathymetric database with 2-minute latitude and longitude resolution was used.

The numerical model is based on a version of the well-known TUNAMI programming code for numerical calculations of tsunami wave propagation [31], in which finite-difference approximations of the linear shallow water equations are undertaken in Mercator projection coordinates [27]:

$$\frac{\partial \zeta}{\partial t} + \frac{\cos\varphi_0}{\cos\varphi}\left[\frac{\partial U}{\partial x} + \frac{1}{\cos\varphi}\frac{\partial (V\cos\varphi)}{\partial y}\right] = 0; \qquad (1)$$

$$\frac{\partial \mathbf{U}}{\partial t} = -\frac{\cos\varphi_0}{\cos\varphi} gh\vec{\nabla}\zeta, \qquad (2)$$

where φ and φ_0 are the current and "mean" latitudes; x, y are the zonal and meridional coordinates, respectively; $\mathbf{U}$ is the horizontal fluid flux vector integrated over depth (h); ζ is the deviation of the free surface from its mean; g is the acceleration due to gravity; and t is time. We solve the Cauchy problem whereby we assume that at the initial time, $t = 0$, the fluid is at rest and the initial deviation of the free surface of the ocean is specified as $\zeta_0(x,y)$. At the free boundary Γ the radiation condition is given by the relation between the normal component of U_n and level ζ:

$$U_n = \zeta\sqrt{gh}, \qquad (3)$$

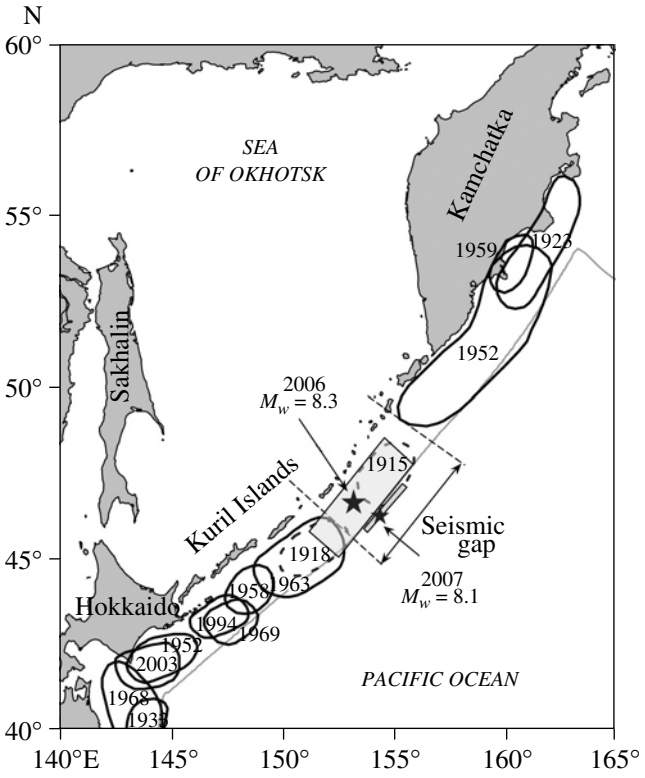

Fig. 2. Source regions of the strongest earthquakes ($M_w \geq 8$) in the Kuril–Kamchatka zone for the period 1900–2005 plotted using different catalogue data: solid lines denote reliable contour lines; dashed lines denote unreliable contour lines; numerals show the year of earthquake occurrence. straight dashed lines denote the limits of the seismic gap in the region of the Central Kuril Islands; asterisks denote epicenters of earthquakes on November 15, 2006 and January 13, 2007; gray rectangles denote the contours of source regions of these earthquakes based on the data in [32, 33]; gray solid line is the axis of the deep Kuril-Kamchatka Trench.

while at the coastal boundary G we specify the zero flux condition:

$$U_n = 0 \text{ at } G. \qquad (4)$$

The calculations were carried out for several scenarios of the hypothetical source with different numbers and types of key-type motions. The details of these calculations are presented in [9, 15]. The time step was chosen to be 2 s, which approximately corresponds to 1/3 of the value required by the Courant stability criterion. A version of the model based on a dipole source region (see the inset in Fig. 3) was selected as the main source region. We further assumed that the source was located along the landward (island) slope of the Kuril-Kamchatka Trench. The total length of the source is about 400 km, and its width is 80 km. The maximum deviations of the sea bottom are +6 m (elevation at the outer "oceanic" side of the dipole source) and –2 m

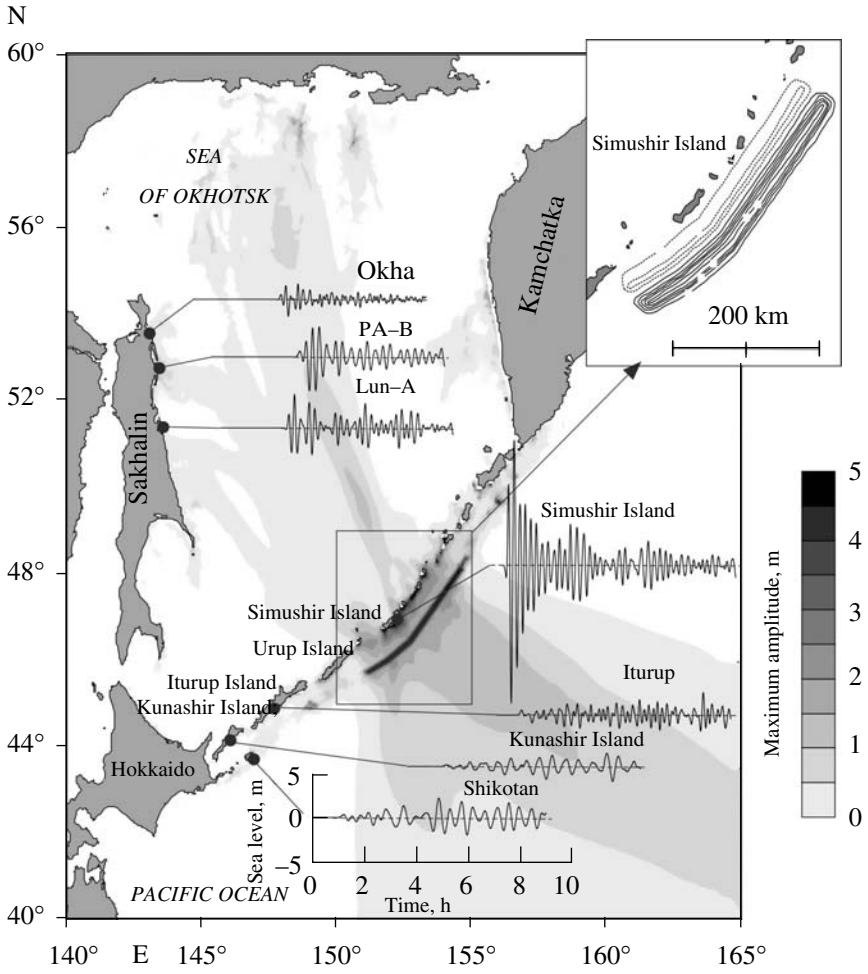

Fig. 3. Maximum simulated amplitudes of a "hypothetical" tsunami with a source in the vicinity of the Central Kuril Islands. The initial tsunami source is shown in the inset (elevation is denoted with solid lines, depression is shown with dashed lines). Simulated tsunami records are shown for different coastal sites of Sakhalin and the Kuril Islands.

(depression at the inner "island" side of the dipole source). This is the "worst realistic" scenario for the source in the sense that all "keys" are active in the "silent zone" of the seismic gap. The scenario is also realistic in terms of our specification of the initial deviation parameters for an $M_w = 8.5$ magnitude earthquake, the magnitude indicated in [9] as most probable.

Results of the model calculations are shown in Fig. 3. According to these findings, the main tsunami energy is directed to the southeast toward the Hawaiian Islands. However, a significant part of the energy also propagates into the Sea of Okhotsk through the deep Bussol and Kruzenstern straits and reaches the eastern coast of Sakhalin Island and major oil- and gas-producing complexes on the shelf. According to the calculations, the heights of tsunami waves at these platforms and pipelines can exceed 4 m (see simulated tsunami records for platforms PA-B (Piltun-Askhotskaya) and Lun-A (Lunskaya) in Fig. 3). It is clear that waves of such height at the Sakhalin coast are a serious threat and would lead to ecological devastation. Tsunami waves propagating to the northwest can reach the Magadan region. These calculations are confirmed by historical data. For example, during the Chilean tsunami of May 22, 1960, a tide gauge in Magadan recorded a maximum tsunami wave height of 267 cm while actual wave heights in Nagayevskaya Bay were observed to exceed 4–4.5 m [7].

A map of the predicted maximum tsunami height distribution (Fig. 3) shows that the highest wave heights should be observed in the immediate vicinity of the source, on the coasts of Simushir, Ketoy, and Matua islands, and on the northern coast of Urup Island.

4. SEISMIC CHARACTERISTICS OF THE EARTHQUAKES OF NOVEMBER 15, 2006 AND JANUARY 13, 2007

The epicenter of the November 15, 2006 ($M_w = 8.3$) earthquake was located on the island slope of the Kuril-Kamchatka Trench (Fig. 1 and 4a). The tsunami source had a dipole shape with seafloor uplift on the outer oceanic side and seafloor depression on the inner (island)

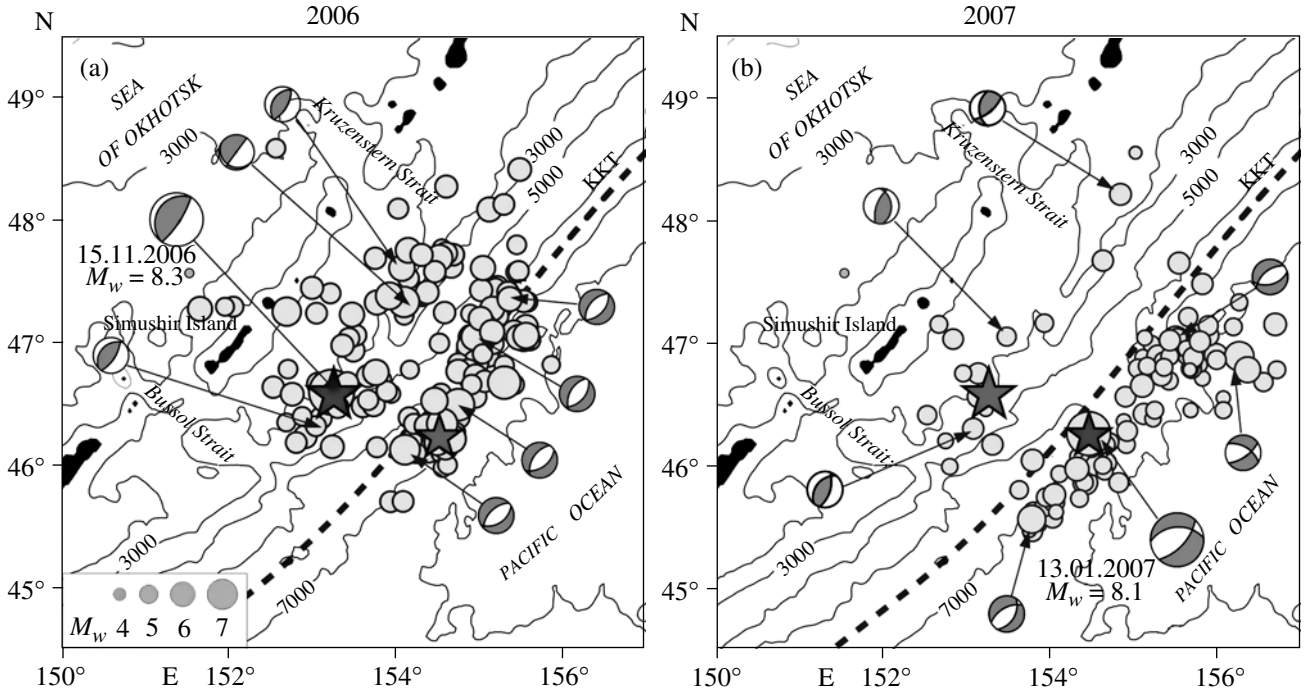

Fig. 4. Distribution of earthquake aftershocks ($mb > 4.5$) for the (a) November 15, 2006 and (b) January 13, 2007 earthquakes for two weeks after the main shocks (aftershocks are indicated with gray circles, whose amplitudes are proportional to their magnitude). The locations of epicenters of the main shocks on November 15, 2006 and January 13, 2007 are marked with asterisks. Source mechanisms are indicated for the main shocks and some strong aftershocks. Thick dashed line shows the axis of the deep Kuril-Kamchatka Trench (KKT). Thin lines show isobaths (m).

side. Thus, the IO RAN forecast [10, 14] and prognostic earthquake model used for the simulation of a hypothetical tsunami [9, 36] (see inset in Fig. 3a) was quite precise. The real earthquake had a slightly smaller displacement amplitude magnitude and a shorter extension (because the northern keys were not activated) and consequently generated a less intense tsunami than was predicted in the "worst scenario". The actual source had a more complex structure than the model source. In contrast to the November event, the epicenter of the main shock of the January 13, 2007 (M_w = 8.1) earthquake was located on the oceanic slope of the Kuril-Kamchatka Trench (Fig. 1 and 4b).

According to data provided by the National Earthquake Information Center (NEIC), the time at the source (T_0) and coordinates of the hypocenters (φ, λ, h) for these two earthquakes were as follows [25]:

(1) November 15, 2006: T_0 = 11:14:13.6 UTC; φ = 46.592°N; λ = 153.266°E; h = 26–30 km;

(2) January 13, 2007: T_0 = 04:23:21.2 UTC; φ = 46.243°N; λ = 154.524°E; h = 10 km.

Estimates of the main energy characteristics of these earthquakes (seismic moment of the source M_0 and earthquake moment magnitude M_w determined from the seismic moment) are presented on the basis of CMT-solutions obtained at Harvard University (USA) [29]:

(1) $M_0 = 3.37 \times 10^{21}$ N m; M_w = 8.3;

(2) $M_0 = 1.65 \times 10^{21}$ N m; M_w = 8.1.

The standard errors of these estimates are $\Delta M_0/M_0 \approx \pm 0.5$, $\Delta M_w \approx \pm 0.2$, therefore the energy released from the elastic deformations of the two earthquakes were of comparable magnitude. However, other seismic characteristics of the two events are significantly different.

The earthquake of November 15, 2006 was felt in populated areas closest to the source: Kurilsk (450 km from the epicenter) and Severo-Kurilsk (500 km from the epicenter) with intensities of 3–4 using the 12 level MSK-64 scale [2]. The second earthquake of January 13, 2007 gave rise to more intense shaking at the same sites: 4–5 in Kurilsk (530 km from the epicenter) and 5–6 in Severo-Kurilsk (500 km from the epicenter) [3]. On the other hand, the earthquake of November 15, 2006 is characterized by a greater number of repeated shocks (535 shocks with magnitude $mb \geq 4.5$ and source depth $h < 40$ km in two months), greater maximum aftershock amplitudes (mb= 6.4), and a greater aftershock distribution area (300 × 220 km^2); the corresponding parameters two months after the earthquake of January 13, 2007 are: 163, 5.8 and 290 × 90 km^2 (Figs. 4a, 4b). The ratio of magnitudes determined from the records of short-period and long-period sensors (mb and M_w) is unusual: for the 2006 earthquake, mb = 6.4, M_w = 8.3 while for the 2007 earthquake, mb = 7.3, M_w = 8.1 [25, 29]. Differences in the earthquake properties explain the aforementioned differences in shock inten-

sity felt at populated sites because they are determined by the short-period component of the source radiation.

The previously noted differences between the earthquakes of November 15, 2006 and January 13, 2007 are due, foremost, to the markedly different tectonics, and consequently different response characteristics, of the two source locations. Figures 4a and 4b show the distribution of aftershock epicenters for both earthquakes for the first 10 days after the main shocks along with the solutions for the source mechanisms for the main shocks and strong aftershocks. Also shown are the displacement amplitudes in the rupture plane obtained within the rupture plane of the spatially finite model [32, 33].

The source of the November 15, 2006 earthquake was located at the front of the island arc at the boundary between the oceanic and continental plates (Fig. 4a). The most probable rupture plane in the source region is located at a depth of 10–25 km and has an area of 400×140 km^2. The rupture plane parallels the axis of the trench (Az = 220°) and slopes gently (15°) toward the island arc [29, 32]. The source has a flat reverse fault motion which is interpreted in the subduction zone as a thrust of the oceanic plate beneath the island arc system. The rupture flank had a maximum displacement of about 9 m, with an accompanying vertical displacement of 2–2.5 m. The aftershock distribution for the November 15, 2006 earthquake (Fig. 4a) defines two main distribution regions: (1) the landward (island) slope of the Kuril-Kamchatka Trench (near the epicenter of the main shock) and (2) the oceanward slope, at the location where the November 13, 2007 earthquake would eventually occur. The two regions are separated by the region of maximum displacement associated with the source of the main shock. The type of motions in the aftershock source regions, which appear under the island and oceanic slopes of the trench, are diametrically opposite: overthrusts occurred in the source region of the November earthquake while exclusively upthrusts were recorded in the source region of the January earthquake. In both cases, the rupture planes were oriented parallel to the axis of the trench.

The January 13, 2007 earthquake originated under the oceanic slope of the trench at a distance of 20 km from the axis of the trench [25] (Fig. 4b). The most probable rupture plane for this earthquake covered an area 200×35 km^2 and extended parallel to the trench axis (Az 43°) at a depth of 9–17 km; it is steeply inclined toward the ocean [29, 33]. The source motion was that of a normal fault (the same as the oceanic aftershocks following the November earthquake); the maximum vertical displacement was about 17 m, and the right-hand (dextral) horizontal displacement was about 11 m. Unlike the aftershocks which followed the November earthquake (Fig. 4a), almost all aftershocks of the January earthquake took place under the oceanic slope of the trench. The maximum number of aftershocks was recorded at distances of 30–70 km from the trench axis. The earthquake of January 13, 2007 was very closely related to the earlier event. The fact that it originated on the oceanic slope of the Kuril-Kamchatka Trench was to a certain extent a consequence of a rebound effect: the earlier earthquake of November 15, 2006 caused a sharp decrease in the compressional stresses at the western extremity of the curved oceanic plate, which eventually led to a repeated fault-type earthquake.

5. TSUNAMI OF NOVEMBER 15, 2006

Immediately after the first seismic information was received on the November 15, 2006 event, it became clear that a particularly strong tsunamigenic earthquake had occurred in the Central Kuril region and that tsunami waves arising from this earthquake could represent a serious threat to the nearby coasts of Russia as well as to the remote regions of the Pacific Ocean. Within two minutes of the earthquake, at 11:16 (hereon, all times are in Coordinated Universal Time, UTC), the Yuzhno-Sakhalinsk Seismic station (YSS) sent urgent information about a major earthquake to the Sakhalin Tsunami Warning Center. At 11:25 (11 minutes after the earthquake), the Center announced a tsunami warning for all the Kuril Islands. According to the YSS data, the preliminary estimate of the magnitude was $M_s = 7.9$, and the corrected estimate was 8.0. The Tsunami Center calculated the time of tsunami arrival at the closest inhabited sites: Malokurilsk at 12:12, Burevestnik (Iturup Island) at 12:21, Severo-Kurilsk at 12:25, and Yuzhno-Kurilsk at 12:40.

At 11:29, the Japan Meteorological Agency (JMA) announced a warning for the northwestern Pacific coast with estimates for the propagation times of the tsunami waves. At 11:30, PTWC (Honolulu, Hawaii) sent preliminary data about the earthquake (M_w = 7.7), announced tsunami warnings for the coasts of Russia and Japan, and transmitted the calculated time of tsunami arrivals for different sites along the coast (in particular, Petropavlovsk-Kamchatskiy at 12:24, Severo-Kurilsk at 12:29, and Ust-Kamchatsk at 12:49). At 12:14, the PTWC upgraded the earthquake to $M_w = 8.1$ and extended the tsunami warning to the Marcus, Wake, and Midway islands, and announced a Tsunami Advisory regime for a number of countries in the Pacific Basin. [2]

The actual heights of tsunami waves at the coast are crucial for tsunami risk estimates. Information from coastal sites closest to the source then makes it possible to give reliable forecasts of wave heights for remote regions. The first eyewitness and instrumental observations of the tsunami arrived at the Sakhalin Center and other centers in approximately 1–1.5 hours after the earthquake. Tsunami waves were observed throughout the region, but no catastrophic wave runup was

[2] Pacific Tsunami Warning Center (PTWC), Honolulu, Hawaii.

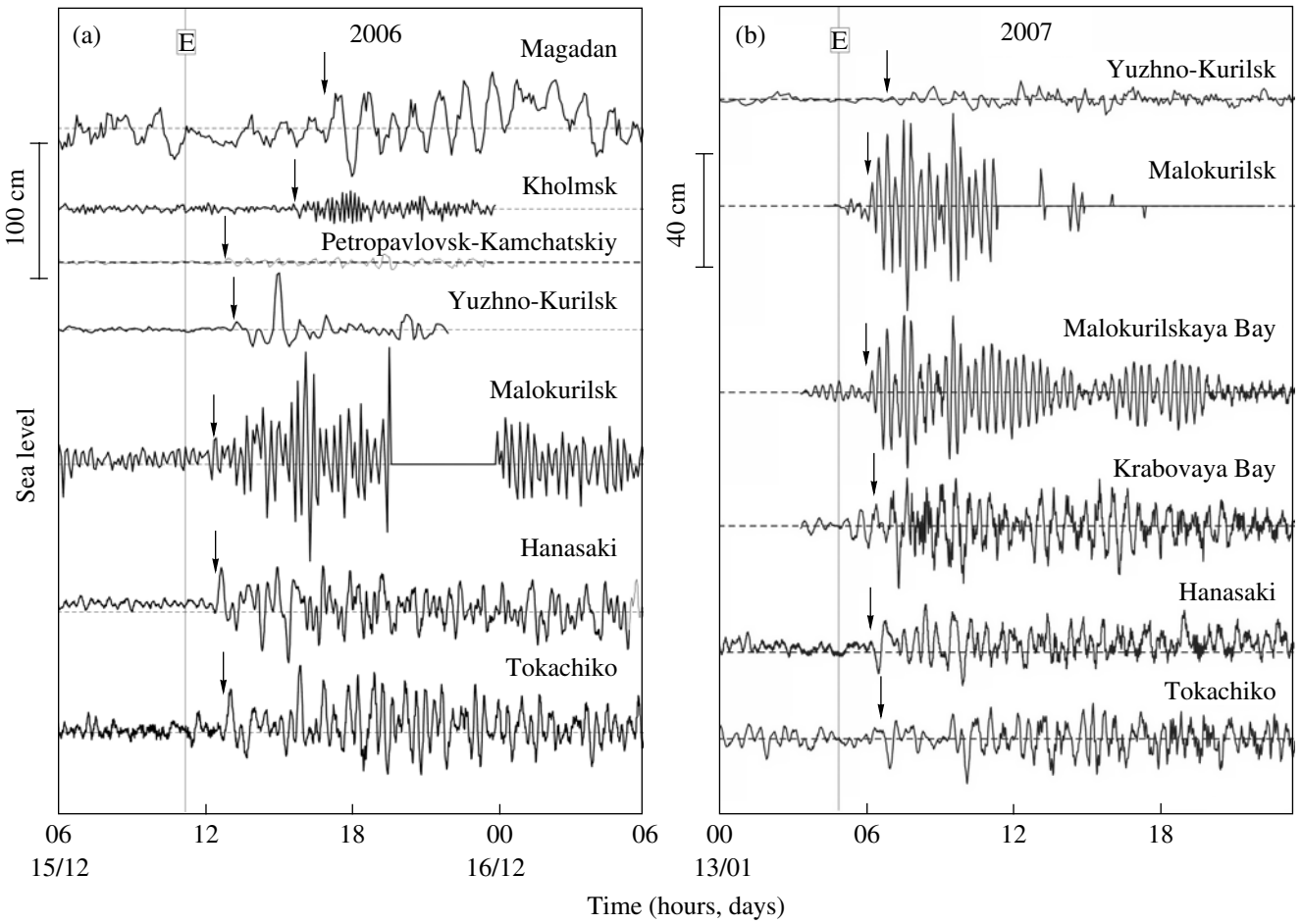

Fig. 5. Tsunami records for the (a) November 15, 2006 and (b) January 13, 2007 events obtained at the Far Eastern coast of Russia and northeastern coast of Hokkaido (Japan). The locations of coastal tide gauges are shown in Fig. 1. The bottom pressure tsunami records were obtained in Malokurilskaya and Krabovaya bays on Shikotan Island. Arrows indicate the moments of arrival of the first tsunami wave; the solid line with the symbol "E" denotes the moments of occurrence of the corresponding earthquakes.

recorded. At 13:19, the Sakhalin Center issued a bulletin to cancel the tsunami warning for the Russian coastline based on eyewitness reports from the Northern and Southern Kuril Islands and primary data about tsunami waves recorded on Hokkaido Island, where the first arriving waves were up to 40 cm high. At 14:58, the PTWC in Honolulu also canceled the tsunami warning. However, later observations showed that the maximum waves hit a majority of the sites 4–6 hours after the first wave. For example, in Malokurilsk, the first wave with a height of approximately 30 cm arrived at 12:22 (i.e., 1 hour 8 min after the earthquake), and the maximum wave (155 cm) was observed at 16:10 (Fig. 5a). A similar long lag for the maximum wave relative to the first wave was recorded everywhere including the coasts of Japan (Fig. 5a), the Hawaiian Islands, California, Chile, New Zealand, etc. [28, 44, 48].

Tsunami waves with a height of order 1 m were recorded at many sites on the coast of Japan (tide gauges in Hanasaki and Tokachiko at the southeastern coast of Hokkaido recorded wave heights of 73 cm; see Fig. 5a), the Hawaiian Islands, California, Oregon, and Mexico. The maximum height (177 cm) was observed at Crescent City (Northern California) where significant damage took place in the port [34, 50]. Damage of ships and port facilities occurred in a number of other sites on the California coast. In regions of the South American coast (Ecuador, Peru, and northern Chile), tsunami waves with heights 80–100 cm were observed.

According to preliminary field data, tsunami waves with heights exceeding 6 m were observed at some sites along the coasts of Simushir and Urup Islands.[3] The maximum oscillations on the Russian coast were recorded by a tide gauge at Malokurilsk. It is possible

[3] In the summer of 2007, the Institute of Marine Geology and Geophysics, Far Eastern Branch of the Russian Academy of Sciences (Yuzhno-Sakhalinsk) in conjunction with IO RAN (Moscow), Moscow State University, the Sakhalin Tsunami Center (Yuzhno-Sakhalinsk), and the University of Washington (Seattle) organized an expedition and conducted a field survey for the coast of the Central Kuril Islands, which showed that at some coastal sites of Simushir, Matua, and some small islands near the Strait of Bussol, observed runup was up to 15 m, and up to 10 m at the northeastern coast of Urup Island [11].

that even stronger oscillations occurred at this station, but the tide gauge was damaged by the tsunami waves and did not function for a few hours (Fig. 5a). Large waves were also recorded by analog tide gauges at Yuzhno-Kurilsk (up to 55 cm), Petropavlovsk-Kamchatskiy (11 cm), Starodubskoye (25 cm), and Kholmsk (24 cm) (Fig. 5a). Fortunately, the Pacific coast of Simushir Island took the brunt of the strongest tsunami wave which to a considerable extent protected the Sakhalin coast and Magadan region. However, as predicted by the prognostic model, part of the tsunami energy propagated into the Sea of Okhotsk through the Bussol and Kruzenstern straits and caused noticeable oscillations in the Magadan region (up to 63 cm based on a tide gauge record; see Fig. 5a). Unfortunately, it was not possible to obtain instrumental estimates of tsunami waves at the northeastern coast of Sakhalin due to the absence of operating tide gauges.

Among the tide gauge records, the most interesting record in terms of analysis is that for Malokurilsk (Fig. 5a). The incoming waves at this station gave rise to monochromatic oscillations with a period of about 18.6 min. Background oscillations with the same period are permanently observed at this station (cf. [17, 41, 45]).

6. TSUNAMI OF JANUARY 13, 2007

At 04:25 UTC on January 13, 2007, the Yuzhno-Sakhalinsk Seismic station (YSS) recorded a major repeated earthquake in the neighborhood of the Central Kuril Islands. A preliminary estimate of the magnitude was $M_s = 8.0$. About 11 minutes later, the YSS station announced a tsunami warning for all Kuril Islands without indicating the coordinates of the earthquake and transmitted this warning to the Sakhalin Tsunami Center. The warning reached inhabited regions in the Kuril Islands at 04:41, five minutes after the announcement of the warning. A tsunami warning system was initiated, and the population located in tsunami hazard zone was evacuated; the vessels were moved to protected harbors and anchorages.

During the earthquake event, the Sakhalin and Pacific tsunami centers were permanently exchanging operative information using a direct telephone connection, which facilitated rapid informed responses and decisions after the announcement of the tsunami warning. At 07:23, the Pacific Tsunami Center canceled the tsunami warning for the entire Pacific region based on the information about sea level changes from the coastal stations in Japan, Alaska, and Russia, as well as from deep-water DART stations in the northwestern part of the Pacific Ocean. At 07:49, the Sakhalin Center also decided to cancel the tsunami warning for the entire Russian coast taking into account the following factors: (1) a lack of significant sea level variations at populated centers on the Kuril Islands within 2–2.5 hours after the calculated tsunami arrival times; (2) a lack of anomalous sea level changes on the Kamchatka coast; and (3) weak tsunami impact at foreign stations (in particular, the coasts of Japan and the Aleutian Islands).

Subsequent observations showed that the earthquake of January 13, 2007 generated a trans-oceanic tsunami, although weaker than the tsunami of November 15, 2006. Noticeable oscillations were recorded by tide gauges on the northern part of the Pacific Ocean: 83 cm at Chichijima Island (Japan); 71 cm at Miyakeshima Island (Japan), 68.5 cm at Shemya Island (Aleutian Islands), and 51 cm at Crescent City and Arena (both in Northern California). In the southern part of the Pacific Ocean, waves with heights of 40 cm were recorded at Easter Island (Chile), of 15–35 cm at the Chilean coast, and 15–20 cm in New Zealand. Maximum wave heights were observed at most sites within a specific time interval after the arrival of the first wave which was similar to that for the tsunami of November 15, 2006.

The relatively poor quality and low signal to noise ratio of the tide gauge records made it impossible for us to identify reliably the tsunami of January 13, 2007 in the tide gauge records from Petropavlovsk-Kamchatskiy, Magadan, and Starodubskoye. The tsunami was accurately recorded only by analog tide gauges in Yuzhno-Kurilsk and Malokurilsk, which are located close to the source. The maximum wave height in the Yuzhno-Kurilsk record was 11 cm (Fig. 5b). As with the 2006 tsunami, the tide gauge record at Malokurilsk is the most interesting. Due to a malfunction in the tide gauge, the record was partly damaged, but the initial 6-hour interval of the record was processable and allowed us to estimate the characteristics of the tsunami waves (Fig. 5b). The first wave arrived at Malokurilsk at 05:32, 1 hour and 9 min after the earthquake, while the maximum wave (72 cm) was observed at 06:53, 1 hour and 21 min after the arrival of the first wave. The first wave was positive at Yuzhno-Kurilsk and Malokurilsk. The first wave was also positive at the Japanese stations located on the northern coast of Hokkaido, while at the Pacific stations Hanasaki, Kushiro, and Tokachiko, as well as at bottom DART stations, the first wave was negative [44].

The tsunami of January 13, 2007 was also clearly recorded by the bottom pressure gauges deployed by the Institute of Marine Geology and Geophysics, Far Eastern Branch of the Russian Academy of Sciences at the end of November 2006 in Malokurilskaya and Krabovaya bays on Shikotan Island (Fig. 5b). The maximum wave height recorded by these gauges was 58 cm in Malokurilskaya Bay and 42 cm in Krabovaya Bay. The bottom pressure record in Malokurilskaya Bay (a bottle-shaped bay with a narrow entrance, see [4, 5, 17]) corresponds closely with the record for the coastal tide gauge: similar to what was observed for the tsunami of November 15, 2006 regular oscillations with a stable period of 18.6 min were recorded. As shown in publications [5, 17], this period is determined by the fundamental eigen Helmholtz mode for Malokurilskaya Bay.

The oscillations in Krabovaya Bay (a long and narrow fjord-like bay) located approximately in eight kilometers from Malokurilskaya Bay were markedly different (Fig. 5b). Specifically, they were slightly less regular, their height was smaller, and the dominant period was about 29.5 min, which is in a good agreement with the period of the fundamental Helmholtz mode and typical period of background oscillations in this bay [41, 45]. The first wave arrived in Krabovaya Bay at 05:41, roughly nine minutes later than in Malokurilskaya Bay.

7. NUMERICAL MODELING OF THE NOVEMBER 15, 2006 AND JANUARY 13, 2007 TSUNAMIS

Numerical modeling of the November 15, 2006 and January 13, 2007 tsunamis was performed using the model discussed in (1)–(4), similar to the prognostic modeling calculations in Section 3, but using the 1-minute GEBCO topography dataset [23] and observed parameters for the tsunami source regions. To estimate the parameters of the 2006 and 2007 tsunami sources we used the results of C. Ji [32, 33] to estimate the parameters of the 2006 and 2007 tsunami sources. Ji used a finite size fracture model to determine the displacements along the rupture plane for these earthquakes. We next used the well-known Okada model [39], which allows the user to transform these displacements into vertical deformations of the sea floor. Within the longwave model typically used for tsunami calculations (for example, [34, 49]), the initial perturbations of the ocean surface in the source region fully coincide with the displacements of the sea floor. However, in the present study, this approach could lead to significant errors because the deformation regions for the 2006 and 2007 earthquakes were comparatively small and the ocean in the source regions quite deep. Therefore, we solved the full Laplace's equation to estimate the initial perturbation of the ocean surface [44]. The sea surface displacements were smooth compared to the longwave approximation of the initial source. In particular, the maximum deviation of the free surface for the source in 2006 decreased from +2.7 to 1.9 m, and for the source of 2007 from –6.8 to –2.6 m. A detailed description of the numerical model is given in [44].

Results of the numerical models for the November 15, 2006 and January 13, 2007 tsunamis are presented in Figures 6 and 7. Figure 6 shows the simulated tsunami records for the same points presented for the "hypothetical" tsunami (Fig. 3). In addition, we added three more locations near Urup, Ketoy, and Paramushir islands, which are interesting for research (Fig. 1). For clarity, the scale of the tide gauge records in Figure 6 was increased five times for six distant locations (Okha, PA-B, Lun-A, Kunashir, Shikotan, and Iturup) compared to the four near-field sites (Urup, Simushir, Ketoy, and Paramushir). Because of the relatively low grid resolution of roughly 1.5 km and the inadequate accuracy of the shelf bathymetry near the coasts of the Kuril Islands, we were unable to obtain a direct comparison of the calculated and observed tide gauge records or obtain exact quantitative estimates of tsunami runup along the coast of the Kuril Islands and Sakhalin. Nevertheless, the calculations give us a clear indication of the general tsunami wave height distributions for the 2006 and 2007 events. The calculations also allow us to intercompare the two events and to compare these events with the results of the prognostic modeling. The spatial maps showing the distribution of maximum amplitudes for the simulated tsunami waves for both events (Fig. 7) give important additional related information.

As predicted (see Fig. 3), the main tsunami energy flux in 2006 and 2007 was directed southeastward toward the Hawaiian Islands and the coast of South America (Figs. 7a, 7b). The wave propagation is clearly affected by the Emperor and Hawaiian submarine ridges. As emphasized in [34, 48], these ridges cause diffraction and reflection of the 2006 and 2007 Simushir tsunami waves. The results of this study agree well with the results in [34, 48] and demonstrate notable variation in the distribution of maximum wave amplitudes in the region.

It is likely that part of the tsunami energy in 2006 and 2007 was trapped by the Kuril shelf and propagated as trapped waves (edge waves [6]) along the Kuril Islands northeastward in the direction of Kamchatka and southwestward toward Japan. It is also likely that the late arrival of the highest waves at Malokurilsk and at some sites on the coast of Japan (Fig. 5) is related to this effect: edge waves at the shelf "conserve" tsunami energy and transport it with minimum loss, but their speed is much lower than the speed of tsunami waves in the open ocean ($c = \sqrt{gh}$), which determines the propagation of the leading tsunami front and first arrival of the waves at coastal sites, as predicted on the basis of the prognostic model (Fig. 3). A smaller fraction of the energy spread into the Sea of Okhotsk through the deep Kruzenstern and Bussol straits (and partly through the other straits of the Kuril Islands) and reached the northeastern coast of Sakhalin Island. According to the numerical calculations, the trough-to-crest height of the tsunami waves in the vicinity of the Lunskaya ocean platform (Lun-A) were as high as 1.5 m during the 2006 event (Fig. 6a) and up to 0.8 m during the 2007 event (Fig. 6b).

According to our calculations, maximum tsunami wave heights occur in the near zone at the coasts of the Simushir and Ketoy islands (Fig. 6), as well as the Matua and Rasshua islands [44]. Calculated tsunami wave heights for the two events in the near zone have similar values, but tsunami wave heights in 2006 appear to have been significantly greater with distance from the source than for 2007. This is confirmed by observations which show that at remote instrumented stations, wave heights for the 2006 and 2007 tsunamis had a ratio of 3 : 1. We associate this effect with differences

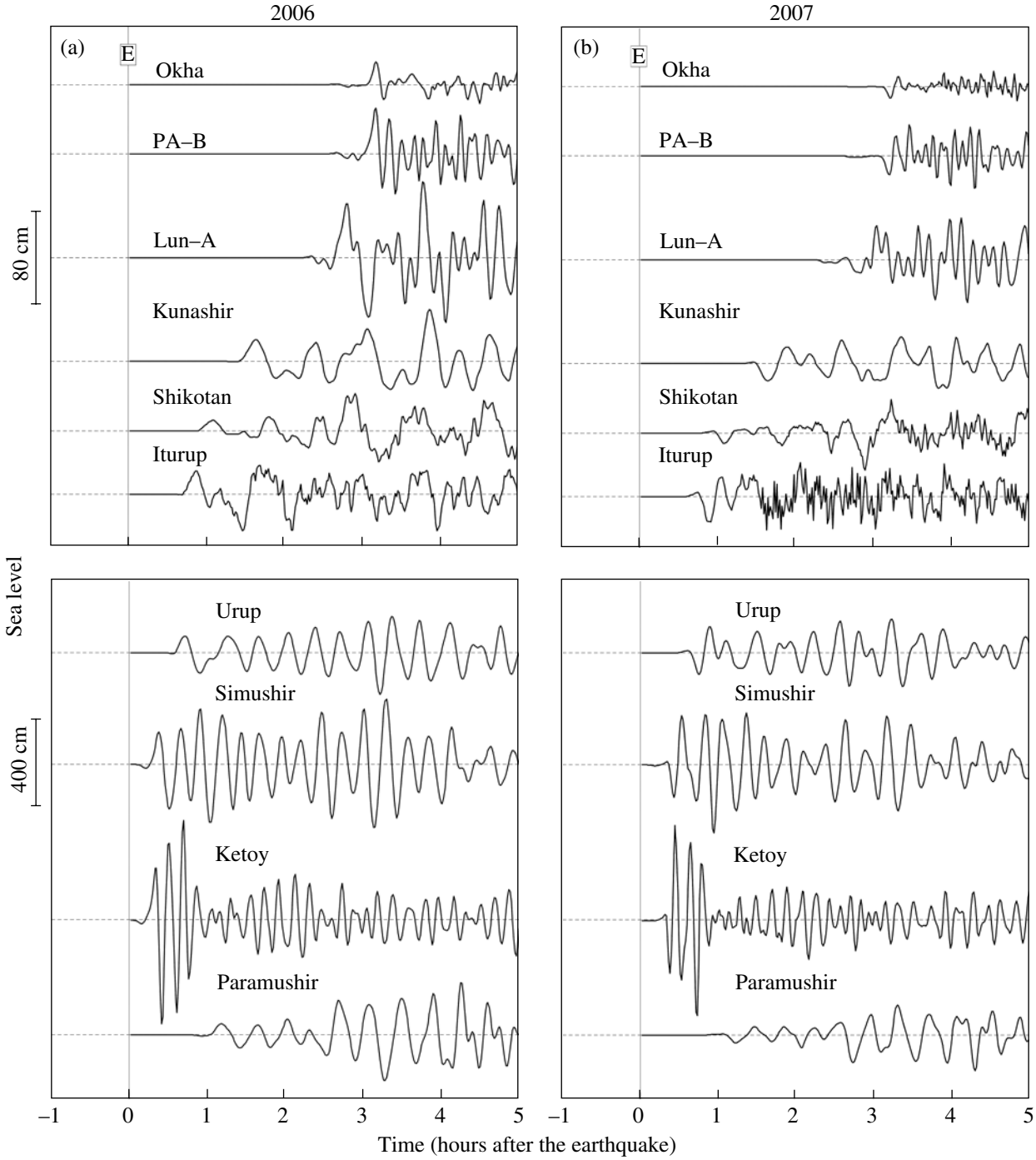

Fig. 6. Simulated records for the tsunamis of (a) November 15, 2006 and (b) January 13, 2007 at different locations along the Sakhalin and Kuril Islands coasts: the locations of sites are shown in Figs. 1 and 3. The solid line with the symbol "E" denotes the moments of the occurrence of the corresponding earthquakes.

in the initial source parameters, specifically the smaller area but more intense earthquake source for the 2007 tsunami. As noted in [44] and clearly shown in Fig. 7, the main lobe of the tsunami wave energy flux for the 2006 tsunami spreads from the source region in a relatively wide beam (Fig. 7a) while that for the 2007 tsunami spreads as a narrow "flood light" beam (Fig. 7b).

Strong differences in the initial phase of the tsunami for two events is an important finding of our calculations: for the 2006 tsunami, the first wave at most sites in Fig. 6 (excluding the sites at Sakhalin) is a positive wave (Fig. 6a), while for the 2007 tsunami it is a negative wave (Fig. 6b). These results agree with observation (Sections 5 and 6) and are related to the aforemen-

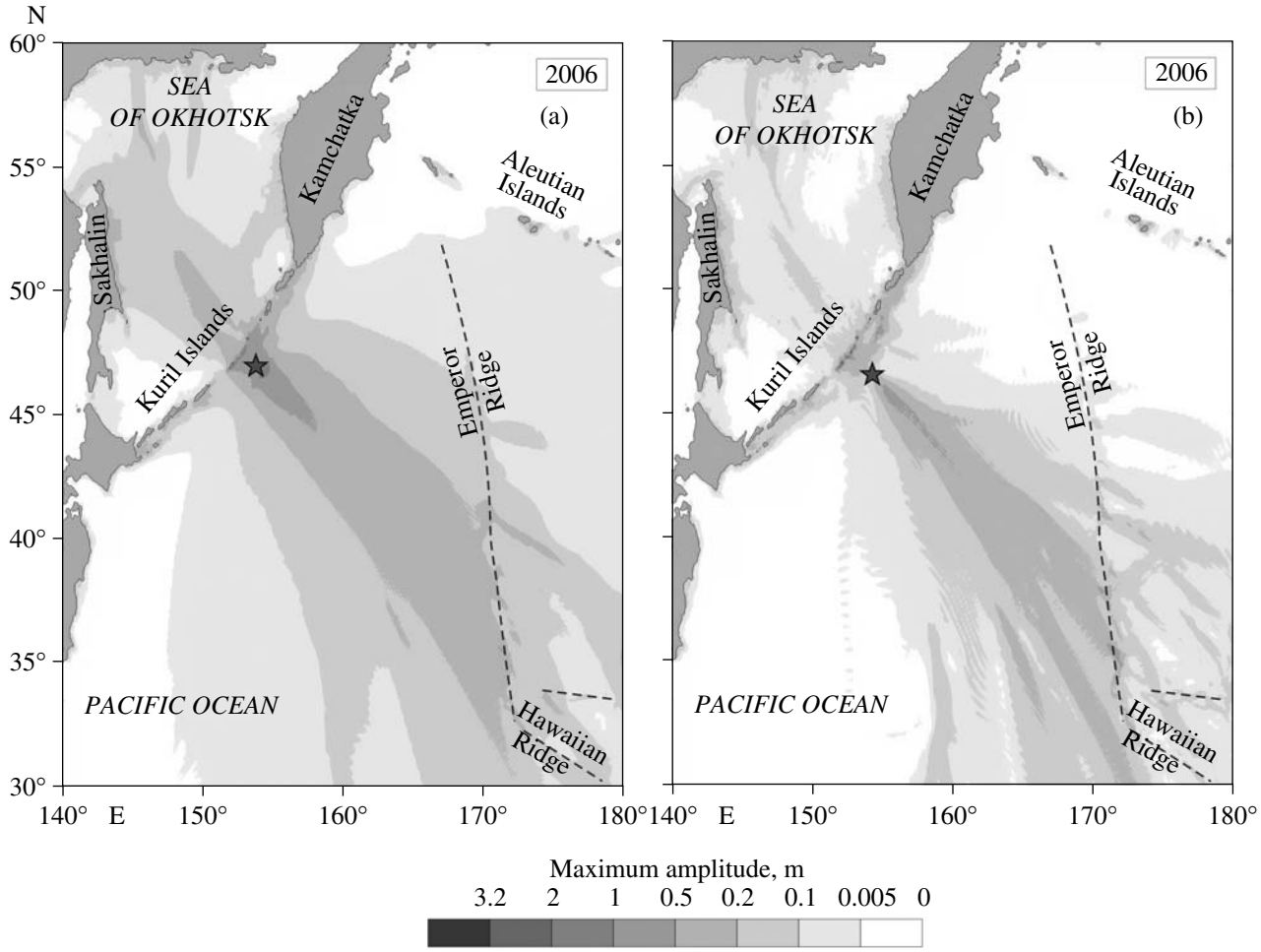

Fig. 7. Numerical simulation of the maximum tsunami amplitudes for the (a) November 15, 2006 and (b) January 13, 2007 events in the northwestern part of the Pacific Ocean and adjacent region of the Sea of Okhotsk. Asterisks denote the locations of the corresponding earthquakes; the thin dashed lines show the Emperor and Hawaiian submarine ridges.

tioned differences (Section 4) in the source parameters: in particular, the source for the 2006 event has seafloor uplift on the oceanic side and depression on the islands side whereas the 2007 event has the opposite sign in seafloor motion, with uplift on the island side and depression on the ocean side (see [44] for a more detailed description of these effects).

One more interesting modeling result is the appearance of high-frequency oscillations sometime after the arrival of the first wave. This effect is more pronounced for the tsunami in 2007. It is especially well defined in the simulated tsunami records for Iturup and Shikotan (Fig. 6b). It clearly manifested in the real tsunami records in 2007 at the coasts of the South Kuril Islands and Japan (see [44, 48] and Fig. 5b). It is likely that these comparatively high-frequency oscillations are related to specific segments of the initial source region, which serve as generators of high-frequency oscillations. Their late arrival is consistent with tsunami wave dispersion (including the dispersion peculiarities of edge waves [6]). Such high-frequency oscillations were observed after the earthquakes of December 26, 2004 and March 28, 2005 in the Indian Ocean (cf., [30]).

8. DISCUSSION AND CONCLUSION

An investigation conducted from 2005 to 2006 showed that the Central Kuril gap consists of four large blocks or "keys" [9, 10, 14]. Seafloor motion associated with the earthquake of November 15, 2006 occurred in the southwestern sector of the seismic gap and involved only two of these blocks. Two blocks on the island side of the continental slope located to the northeast of the source region were not affected by this motion. As a result, the undisturbed northeastern sector of the seismic gap (not previously impacted by major earthquakes) remains a possible zone for a future $M_w \geq 8$ event. The situation in the Indian Ocean had developed

along the same lines. In particular, the catastrophic earthquake of December 26, 2004 (M_w = 9.3) affected the source zone that extended over 1300 km in the northern part of the Sunda Islands Arc; the source zone of the destructive earthquake that followed on March 28, 2005 (M_w = 8.7) was located immediately to the south of the first earthquake source [40].

Analysis of the seismic characteristics of the November 15, 2006 earthquake demonstrates that this was an inter-plate event, and that its source region was limited by transverse transform fractures passing through the Bussol and Kruzenstern straits [10, 12]. Comparison of the maximum displacement (9 m) in the earthquake source region with the mean velocity of convergence of the Pacific and Okhotsk plates in this region (87 mm/yr) [22] gives an approximate estimate of once every 100 years for the recurrence of an earthquake with this displacement amplitude. The earthquake of January 13, 2007 (second event) with M_w = 8.1 was directly linked to the previous earthquake, and was also an intra-plate event. Such earthquakes frequently occur in subduction zones at the outer slope of the trench during times when there is intense tension of the curved oceanic plate near the trench axis following a strong inter-plate earthquake. Unlike the November 15, 2006 event, the January 13, 2007 earthquake has a dominant normal fault motion beneath the oceanic slope of the trench and specific oceanward horizontal displacement of the aftershock epicenter region. Peak activity following the November 15, 2006 earthquake was observed at the outer slope of the trench near the axis, whereas the majority of repeated aftershocks following the January 13, 2007 earthquake took place under the ocean bottom at distances of 30–70 km from the axis of the trench.

Thus, the events on November 15, 2006 with M_w = 8.3 and January 13, 2007 with M_w = 8.1 are closely linked and together represent one of a series of episodes in the long history of oceanic plate subduction under the Kuril-Kamchatka Island Arc.

We note that strong earthquakes in the relatively unpopulated regions of the Central Kuril Islands are not a hazard in themselves but can generate destructive tsunami waves, which could cause catastrophic consequences for the Far Eastern coast of Russia, and especially for the northeastern coast of Sakhalin Island. This was the reason that, in the spring of 2005 (one and a half years before the actual events), we undertook prognostic numerical simulations of tsunamis that might be generated within the expected earthquake region [9, 36]. We considered the most possible earthquake scenario, which (on a somewhat reduced scale) was eventually realized by the earthquake of November 15, 2006. The results of the prognostic model calculations correspond qualitatively to the actual tide gauge observations at the coast and in the open ocean, as well as to the preliminary field survey data collected in expeditions on the coast of the Kuril Islands during the summer of 2007 [11]. This successful outcome supports the high potential for prognostic tsunami modeling for regions of anticipated seafloor earthquakes.

Both Simushir earthquakes were tsunamigenic and resulted in strong but not catastrophic tsunamis, which were recorded over the entire Pacific basin. The tsunamis of November 15, 2006 and January 13, 2007 were generated in the same region and had many common features: transoceanic propagation, a southeastward directed energy radiation, observed dominant wave periods from 2–3 to 15–20 min, and long lag times (excluding the very near zone) of the maximum wave heights relative to the arrival time for the first wave. On the other hand, there were marked differences in the earthquake source mechanisms which led to important and interesting differences in the characteristics of the tsunamis at the coast [44].

The main difference in the tsunamis is in the sign of the first wave arrival. For the 2006 tsunami, a leading positive wave radiated to the open ocean and a leading negative wave propagated to the nearest coast, i.e. toward the Kuril Islands. This scenario is typical for many strong tsunamis and, in particular, was observed for the catastrophic tsunami of December 26, 2004, when the lead positive wave propagated into the Indian Ocean and the lead negative wave to the nearest coast. When we performed prognostic calculations of the tsunami generated within the Central Kuril seismic gap, this was considered the most probable scenario to model (Section 3). The sign of the first wave and parameters of the actual November 15, 2006 tsunami were very close to the parameters of the "hypothetical tsunami", although the area of the actual source appeared smaller than the calculated one, while the tsunami was weaker than anticipated according to the worst case source development scenario. For the 2007 tsunami, the opposite situation was observed: the first positive wave was directed toward the Kuril Islands, while the first negative wave propagated into the Pacific Ocean.

The 2007 tsunami was weaker (it is likely that the bottom motion during the earthquake was a strike slip fault not an upthrust fault as was the case for 2006 earthquake) and did not lead to destructive waves for remote inhabited sites similar to those caused by the 2006 tsunami in Crescent City (California). At the same time, the 2007 tsunami appeared more focused (owing to a smaller source area and greater maximum seafloor displacement in the source region): the main tsunami energy radiated in a narrower beam. Hence, according to our numerical simulations, the 2007 tsunami led, in the near zone, to effects that were not weaker than those for the 2006 tsunami. The differences in the areas of the sources and in their location (the 2006 source was larger and located closer to the coast) led to additional differences: trapping of wave energy over the shelf for the 2006 tsunami was considerably stronger than for the 2007 tsunami. At the same time, the smaller source

area and greater amplitude seafloor motion in the source area of the 2007 tsunami led to the generation of higher frequencies in the tsunami wave spectrum and to stronger wave dispersion.

The Simushir tsunamis of 2006 and 2007 appear to be mirror images of the Chilean tsunami of May 22, 1960 (although they were much weaker): in 1960, tsunami waves generated at the coast of Chile crossed the Pacific Ocean and struck the coasts of the Kuril Islands and Japan, while in November 2006, significant tsunami waves from the Kuril region reached the coast of Chile.

Unfortunately, our ability to accurately detect tsunami waves on the coasts of Russia and, correspondingly, our capacity for providing operational corrections to tsunami warnings are highly limited due to the lack of the necessary instruments: digital tide gauges with real-time signal transmission. Sea level measurements in the Far East of Russia are currently performed by a few archaic analog tide gauges. The closest tide gauges to the epicenters of earthquakes on November 15, 2006 and January 13, 2007 were located 500–800 km away at Malokurilsk, Yuzhno-Kurilsk, and Petropavlovsk-Kamchatskiy. According to modern requirement for operational tsunami service, the spatial distribution of tide gauges at seismically active coasts should be of the order of 100–150 km. The lack of earthquake and tsunami monitoring systems on a real time basis, the lack of information concerning tsunamis at coasts closest to the epicenter of earthquakes (Urup, Simushir, Matua, and other islands), and the impossibility of performing visual observations in the dark (the first Simushir earthquake occurred at night) created extreme difficulties for the operational tsunami warning services during the 2006 and 2007 events.

The two strong tsunamis generated at the Far Eastern coasts of Russia demonstrate once again the serious risk of this phenomenon to the Russian coast. In past years, this hazard became even greater due to the intense development of oil and gas producing industries, laying of pipelines, construction of terminals, and so on in Sakhalin. A destructive tsunami could lead to a serious ecological disaster in this region. This also leads to sharp increase in the cost of false tsunami alarms. The Shikotan tsunami of 1994 is an example: a false tsunami alert on the Hawaiian Islands related to this tsunami led to the loss of two human lives and caused damage of 70 million dollars.[4] Permanent monitoring of tsunami waves and associated hazards in such situations becomes an important social-economical problem. Deployment of modern digital tide gauges at the coasts of the Kuril Islands, Kamchatka, and Sakhalin, the deployment of bottom sea level stations, and bottom seismographs near the coasts and in the open ocean should become a top-priority.

[4] Private communication of Laura Kong, International Information Tsunami Center, Honolulu, 2006.

ACKNOWLEDGMENTS

This study was supported by the Russian Foundation for Basic Research (project nos. 05-05-64585, 06-05-08108, and 08-05-00909).

REFERENCES

1. E. Geist, V. Titov, and K. Sinolakis, "Tsunami: Wave of Change," Scientific American, No. 5, 32–39 (2006).
2. Geophysical Service of the RAS. Information about a Strong Earthquake in the Central Part of the Kuril Islands on November 15, 2006, http://www.ceme.gsras.ru/cgi-bin/info_quake.pl?mode = 1&id = 89.
3. Geophysical Service of the RAS. Information about a Strong Earthquake in the Central Part of the Kuril Islands on January 13, 2007, http://www.ceme.gsras.ru/cgi-bin/info_quake.pl?mode = 1&id = 92.
4. V. A. Djiumagaliev, E. A. Kulikov, and S. L. Soloviev, "Analysis of Fluctuations in Sea Level in Little Kuril Bay due to the Tsunami of February 16, 1991," Atmosph. Oceanic Phys., **29** (6), 812–818 (1993); Izv. Akad. Nauk, Fiz. Atmos. Okeana **29** (6), 848–854 (1993).
5. V. A. Djumagaliev, A. B. Rabinovich, and I. V. Fine, "Theoretical and Experimental Estimation of Transfer Peculiarities of the Malokurilsk Bay Coast, the Island of Shikotan," Atmosph. Oceanic Physics, **30** (5), 680–686 (1994); Izv. Akad. Nauk, Fiz. Atmos. Okeana **30** (5), 711–717 (1994).
6. V. V. Efimov, E. A. Kulikov, A. B. Rabinovich, and I. V. Fine, *Waves in Boundary Regions of the Ocean* (Gidrometeoizdat, Leningrad, 1985) [in Russian].
7. Kh. S. Kim and A. B. Rabinovich, "Tsunami on the Northwestern Coast of the Sea of Okhotsk," in: *Natural Catastrophes and Nature Disasters in the Far Eastern Region* (DVO AN SSSR, Vladivostok, 1990), pp. 206–218 [in Russian].
8. E. A. Kulikov, A. B. Rabinovich, and R. E. Thomson, "On Long-Term Tsunami Forecasting," Okeanologiya **45** (4), 544–556 (2005) [Oceanology **45** (4), 488–499 (2005)].
9. N. P. Laverov, S. S. Lappo, L. I. Lobkovsky, and E. A. Kulikov, "Strongest Underwater Earthquakes and Catastrophic Tsunamis, Analysis, Modeling, Forecast," in: *Fundamental Investigations of Oceans and Seas* (Nauka, Moscow, 2006), No. 1, pp. 191–209 [in Russian].
10. N. P. Laverov, S. S. Lappo, L. I. Lobkovsky, *et al.*, "The Central Kuril Gap": Structure and Seismic Potential, Dokl. Earth Sci. **409**, 787–790 (2006) [Dokl. Akad. Nauk **408**, 1–4 (2006)].
11. B. V. Levin, V. M. Kaistrenko, A. V. Rybin, *et al.*, "Manifestations of the Tsunami on November 15, 2006, on the Central Kuril Islands and Results of the Runup Heights Modeling," Dokl. Earth Sci. **419**, 335–338 (2008) [Dokl. Akad. Nauk **419**, 118–122 (2008)].
12. L. I. Lobkovsky, *Geodynamics of Spreading and Subduction Zones, Two-Level Plate Tectonics* (Nauka, Moscow, 1988) [in Russian].

13. L. I. Lobkovsky, "A Wave of Complete Destruction," V Mire Nauki, No. 5, 74–81 (2005).

14. L. I. Lobkovsky, "Catastrophic Earthquake and Tsunami of December 26, 2004 in the Northern Part of the Sunda Islands Arc: Geodynamical Analysis and Similarity with the Central Kuril Islands," Vestnik RAEN, No. 2, 53–61 (2005).

15. L. I. Lobkovsky, R. Kh. Mazova, L. Yu. Kataeva, and B. V. Baranov, "Generation and Propagation of Catastrophic Tsunamis in the Sea of Okhotsk Basin: Possible Scenarios," Dokl. Earth Sci. **410**, 1156–1159 (2006) [Dokl. Akad. Nauk **410**, 528–531 (2006)].

16. L. I. Lobkovsky, E. A. Kulikov, A. B. Rabinovich, *et al.*, "Earthquakes and Tsunamis (November 15, 2006, and January 13, 2007) in the Central Kuril Islands Region: A Justified Prediction," Dokl. Earth Sci. **419**, 320–324 (2006) [Dokl. Akad. Nauk **418**, 829–833 (2006)].

17. A. B. Rabinovich and A. S. Levyant, "Influence of Seiche Oscillations on the Formation of Long-Wave Spectrum near the Coast of the Southern Kuriles," Oceanology **32** (1), 17–23 (1992).

18. S. L. Soloviev and Ch. N. Go, *Catalogue of Tsunamis of the Western Shore of the Pacific Ocean* (Nauka, Moscow, 1974) [in Russian] (Canadian Transl. Fish. Aquatic Sci., No. 5077, Ottawa (1981) [Engl. Transl.]).

19. S. L. Soloviev and E. A. Kulikov, "Restoring the Parameters for the Origin of Tsunamis from the Spectral Characteristics of Waves at the Shore," Atmosph. Oceanic Phys. **23** (1), 66–71 (1987).

20. S. A. Fedotov, *Regularities in the Distribution of Strong Earthquakes in Kamchatka, Kuril Islands, and Northwestern Japan*, Tr. In-ta Fiziki Zemli AN SSSR **203** (36), 66–93 (1965).

21. S. A. Fedotov, *Long-Term Seismic Forecast for the Kuril-Kamchatka Arc* (Nauka, Moscow, 2005) [in Russian].

22. P. Bird, "An Updated Digital Model of Plate Boundaries," Geochemistry, Geophysics, Geosystems **4** (3) (2003).

23. *British Oceanographic Data Centre: GEBCO Digital Atlas*, (2003).

24. D. H. Christensen and L. J. Ruff, "Outer-Rise Earthquakes and Seismic Coupling," Geophys. Res. Lett. **10** (8), 697-700 (1983).

25. Earthquake Center, USGS, http://earthquake.usgs.gov/eqcenter/; ftp://hazards.cr.usgs.gov/.

26. E. R. Engdahl and A. Villasecor, *International Handbook of Earthquake and Engineering Seismology*, ed. by W. H. K. Lee et al., Part A, Ch. 41, (Academic Press, 2002), pp. 665–690.

27. I. V. Fine, A. B. Rabinovich, R. E. Thomson, *et al.*, "The Grand Banks Landslide-Generated Tsunami of November 18, 1929, Preliminary Analysis and Numerical Study," Marine Geol. **215**, 45–57 (2005).

28. Y. Fujii and K. Satake, "Tsunami Sources of November 2006 and January 2007 Great Kuril Earthquakes," Bull. Seism. Soc. Amer. 2008. **98** (3), 1559–1571.

29. Global CMT Web Page, http://www.globalcmt.org/.

30. J. A. Hanson, C. L. Reasoner, and J. R. Bowman, "High-Frequency Tsunami Signals of the Great Indonesian Earthquakes of 26 December 2004 and 28 March 2005," Bull. Seism. Soc. Amer. **97** (1A), S232–S248 (2007).

31. F. Imamura, "Review of Tsunami Simulation with a Finite Difference Method," in *Long-Wave Runup Models*, Ed. by H. Yeh et al., (World Scientific, River Edge, NJ, 1995), pp. 43–87.

32. C. Ji, "Rupture process of the November 15, 2006 Magnitude 8.3 Kuril Island Earthquake" (http://earthquake.usgs.gov/eqcenter/eqinthe news/2006/usvcam/finite_fault.php).

33. C. Ji, "Rupture Process of the January 13, 2007 Magnitude 8.1 Kuril Island Earthquake" (http://earthquake.usgs.gov/eqcenter/eqinthe news/2007/us2007xmae/finite_fault. php).

34. Z. Kowalik, J. Horillo, W. Knight, and T. Logan, "The Kuril Islands Tsunami of November 2006: Part I: Impact at Crescent City by Distant Scattering," J. Geophys. Res. **113**, C01020 (2008).

35. E. A. Kulikov, A. B. Rabinovich, and R. E. Thomson, "Estimation of Tsunami Risk for the Coasts of Peru and Northern Chile," Natural Hazards **35** (2), 185–209 (2005).

36. L. Lobkovsky and E. Kulikov, "Analysis of Hypothetical Strong Earthquake and Tsunami in the Central Kuril Arc," Geophys. Res. Abstracts **8**, 04138 (2006): SRef-ID: 1607-7962/gra/EGU06-A-04138.

37. W. R. McCann, S. P. Nishenko, L. R. Sykes, and J. Krause, "Seismic Gaps and Plate Tectonics: Seismic Potential for Major Boundaries," Pure Appl. Geophys **117**, 1082–1147 (1979).

38. S. P. Nishenko, "Circum-Pacific Seismic Potential 1989–1999," Pure Appl. Geophys **135**, 169–259 (1991).

39. Y. Okada, "Surface Deformation Due to Shear and Tensile Faults in a Half-Space," Bull. Seism. Soc. Amer. **75**, 1135–1154 (1985).

40. F. F. Pollitz, P. Banerjee, R. Bürgmann, *et al.*, "Stress Changes along the Sunda Trench Following the 26 December 2004 Sumatra-Andaman and 28 March 2005 Nias Earthquakes," Geophys. Res. Lett. **33**, L06309 (2006).

41. A. B. Rabinovich, "Spectral Analysis of Tsunami Waves: Separation of Source and Topography Effects," J. Geophys. Res. **102** (C6), 12663–12676 (1997).

42. A. B. Rabinovich, V. A. Djumagaliev, I. V. Fine, and E. A. Kulikov, "Analysis of Weak Tsunamis in the Region of Kuril Islands and Resonance Influence of Topography," *Proc. IUGG / IOC Int. Tsunami Symposium*, Wakayama, Japan, pp. 95–105 (1993).

43. A. B. Rabinovich, E. A. Kulikov, and R. E. Thomson, "Tsunami Risk Estimation for the Coasts of Peru and Northern Chile," *Proc. ITS CD* (2001), Session 1, No. 1–5, pp. 281–191.

44. A. B. Rabinovich, L. I. Lobkovsky, I. V. Fine, *et al.*, "Near-Source Observations and Modeling of the Kuril Islands Tsunamis of 15 November 2006 and 13 January

2007," Advances in Geosciences **14** (1), 105–116 (2008).

45. A. B. Rabinovich and S. Monserrat, "Generation of Meteorological Tsunamis (Large Amplitude Seiches) near the Balearic and Kuril Islands," Natural Hazards **18** (1), 27–55 (1998).
46. W. H. F. Smith and D. T. Sandwell, "Global Sea Floor Topography from Satellite Altimetry and Ship Depth Soundings," Science **277** (5334), 1956–1962 (1997).
47. S. Stein and E. A. Okal, "Speed and Size of the Sumatra Earthquake," Nature **434**, 581–582 (2005).
48. Y. Tanioka, Y. Hasegawa, and T. Kuwayama, "Tsunami Waveform Analyses of the 2006 Underthrust and 2007 Outer-Rise Kuril Earthquakes," Advances in Geosciences **14**, 129–134 (2008).
49. V. V. Titov, A. B. Rabinovich, H. Mofjeld, *et al.*, "The Global Reach of the 26 December 2004 Sumatra Tsunami," Science **309** (1), 2045–2048 (2005).
50. B. Uslu, J. C. Borrero, L. A. Dengler, and C. E. Synolakis, "Tsunami Inundation at Crescent City, California Generated by Earthquakes Along the Cascadia Subduction Zone," Geophys. Res. Lett. **34**, L20601 (2007).